Modeling growth of one-dimensional islands: Influence of reactive defects

Pavel Kocán,* Pavel Sobotík, Ivan Ošťádal, Martin Setvín, and Stanislav Haviar
Charles University in Prague, Faculty of Mathematics and Physics, Department of Surface and Plasma Science, V Holešovičkách 2, 180 00 Prague 8, Czech Republic
(Received 29 July 2009; published 22 December 2009)

Influence of reactive defects on size distribution of one-dimensional islands is studied by means of kinetic Monte Carlo simulations in combination with an analytical approach. Two different models are examined: a model with anisotropically diffusing atoms irreversibly aggregating to islands, and a reversible model close to thermal equilibrium which allows atom detachment from islands during the growth. The models can be used to simulate island growth of group III metals deposited on the Si(100)2×1 surface at room temperature: Al, Ga (irreversible model), and In (equilibrium model). We demonstrate that concentration of the reactive defects 0.0025 per site may change the island size distribution from monomodal to monotonically decreasing in the case of the irreversible model. At concentration $\geq$0.005 defects per site, a difference between results of the studied models is suppressed by the influence of the defects and similar island size distributions are obtained.

DOI: 10.1103/PhysRevE.80.061603 PACS number(s): 81.15.Aa, 87.10.Rt, 68.55.ag

I. INTRODUCTION

Anisotropy of crystal surfaces often results in growth of one-dimensional (1D) nanostructures upon deposition of mobile adatoms. Formation of such single-atom-wide islands is a subject of both experimental [1–7] and theoretical [3,7–12] research as a model of 1D self-organization. Experimentally, the scanning tunneling microscopy (STM) provided island size distributions for several systems of 1D islands [3,7,8]. Various theoretical approaches were used to explain the experimentally quantified morphologies: kinetic Monte Carlo (kMC) simulation [3,8,10,13], rate equations [11], and analytical derivation from thermodynamic consideration [10].

Besides other systems of 1D assembling, group III metal atoms deposited on the Si(100)2×1 surface attracted attention. In this case, formation of 1D chains of dimerized atoms was explained by a surface mediated reaction [14]. Experiments showed that islands composed of group III atoms with larger atomic radii (In, Tl) are unstable at room temperature [1,2,4,15], while those with smaller atomic radii (Al, Ga) form stable islands [3,14]. Based on STM observation, Albao *et al.* reported monotonically decreasing size distribution (MDSD) of Ga islands grown on the Si(100)2×1 surface [3]. Such a form of the distribution is rather surprising, because in the case of low-coverage irreversible island growth, generally monomodal distribution is expected, independently on island geometry [16,17]. Albao *et al.* interpreted the MDSD by means of kMC simulations using an irreversible model with strong anisotropy in combination with presence of so-called prohibited zones along islands (Fig. 1). Later, their experimental data [3] were interpreted by Tokar and Dreyssé [10] by using a qualitatively different model. In the latter case, the MDSD was obtained as a result of reversible growth under thermal equilibrium. This model contains one parameter only—metal atom pair interaction energy between the nearest neighbors in a metal chain. By fitting this single parameter Tokar and Dreyssé [10] obtained the same statistics as measured by Albao *et al.*

Even though perfect periodic surface of a crystal is commonly used in theoretical studies, defects are always present on real surfaces. The defects can be classified as line (e.g., step edges, domain boundaries) or point defects (e.g., molecules of adsorbate, step kinks, missing atoms); reactive (acting as nucleation centers) or inert with respect to adsorbed atoms. Especially in the case of highly mobile adsorbate, all stages of growth may be governed by presence of defects, as demonstrated for growth of two-dimensional islands [18]. Therefore, it is important to understand how various defects influence surface adsorption, nucleation and growth of nanostructures.

In the case of the Si(100)2×1 surface, *C*-type defects, interpreted as dissociated water molecules [19–21], are commonly observed on the substrate. It was demonstrated both by experiments and *ab initio* calculations [4,15,22,23] that the *C*-type defects represent preferred nucleation sites for deposited atoms. For the first time, the *C* defects were accounted for in simulations in Ref. [13] in the case of irreversible model applied to Ga growth on Si(100)2×1. A reversible model taking into account nucleation on defects was recently used to simulate growth of In islands on the Si(100)2×1 surface [8]. However, role and impact of the defects remained under discussion [8,13,22]. Another example of point defects pinning 1D islands can be found at

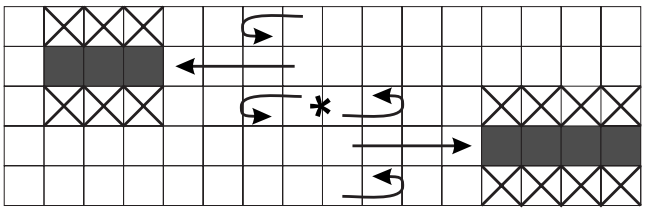

FIG. 1. A schematic illustration of a model with prohibited zones (crosses) along islands (shaded). Mobility of metal adatoms is much higher in direction parallel with 1D islands than in perpendicular direction. The arrows indicate tendency of adatoms either to be attached to island ends or repelled from the prohibited zones. The asterisk marks the position where a single adatom is trapped between two prohibited zones.

*pavel.kocan@mff.cuni.cz

adsorption of metal atoms on vicinal Pt surface [5–7]. On Pt surface, step edges are decorated by diffusing adatoms, assembling to 1D islands along step edges. Step kinks, representing the most stable sites for deposited atoms, play a role of the reactive defects.

Here, we analyze an influence of reactive defects on low coverage growth (<0.1 monolayer, ML) of 1D atomic islands. Two different models are studied, irreversible and close-to-equilibrium one, respectively. The goal was to diminish number of parameters without loosing accuracy. As a result, important processes are identified and risk of "correct" results obtained by an "incorrect" simulation with too many parameters is reduced. From the irreversible model, we extracted important processes and defined a simple model utilizing capture zones. A model with diffusion restricted to one dimension, which reflects the surface anisotropy, is tested. For the close-to-equilibrium model we solved equilibrium conditions taking into account nucleation on defects and neglecting diffusion pathways. The approximative methods are compared to "exact" results of kMC simulations.

We use growth of the group III metals deposited on the Si(100)2×1 surface with *C*-type defects as an example of growth of 1D islands strongly influenced by reactive defects. However, such an approach can be easily adopted to other systems with growth of 1D objects.

II. MONTE CARLO IMPLEMENTATION

A kMC implementation of the standard activation dynamics [17] was used for simulations. A lattice was orthogonal with occupancy of each cell equal to zero or one. In the model, anisotropy is included by means of distinguished directions perpendicular ($\perp$) and parallel ($\parallel$) with respect to orientation of 1D islands, respectively. Rates $\nu_{\perp,\parallel}$ of hopping processes were calculated using equation

$$\nu_{\perp,\parallel} = \nu_0 \exp\left(\frac{-E_{\perp,\parallel}}{kT}\right), \tag{1}$$

where ν_0 is the frequency prefactor, k is the Boltzmann constant, and T is the temperature. Activation energies for jumps in both directions are calculated at each position occupied by an adatom with respect to the nearest neighbors (NN),

$$E_{\perp,\parallel} = E^0_{\perp,\parallel} + N_{\parallel}E_{attr} - N_{\perp}E_{rep} + N_{D\parallel}E_{attrD}, \tag{2}$$

where $E^0_{\perp,\parallel}$ is the energy barrier for a jump of an isolated atom in the direction perpendicular or parallel to island orientation, respectively; $N_{\perp,\parallel}$ is number of NN in perpendicular and parallel direction, respectively; E_{attr} is the attractive energy of a bond within a 1D island; E_{rep} is the repulsion energy in positions along islands; $N_{D\parallel}$ is a number of NN reactive defects in the parallel direction and finally E_{attrD} is the bonding energy between a defect and adatom. A similar model [except for the last term in Eq. (2)] was previously used for simulations on the defect-free lattice [10].

One-dimensional islands composed of group III metals are not formed in the nearest neighborhood in $\perp$ direction, but are separated at least by a distance of $2a$, where $a=0.384$ nm is surface unit cell spacing. This can be explained by lack of dangling bonds on the sites neighboring to the positions occupied by an island. There are two possible ways how to include this feature easily into a model. First, by means of prohibited zones, which exclude $NN_{\perp}$ positions along 1D islands from diffusion pathways. Diffusion restricted by the prohibited zones and by strong anisotropy is schematically illustrated in Fig. 1. Second possibility is to decrease dramatically adatom lifetime at the $NN_{\perp}$ sites, which practically excludes nucleation of islands with spacing $1a$. Observation of adsorbate dynamics on In deposited Si(100)2×1 surface at regime close to saturation coverage (0.5 ML) indicates that mobile adatoms can overcome occupied and prohibited zones [15]. So far there is no experimental evidence of a real mechanism at low coverage available. Therefore, we tested both suggested possibilities.

In all presented kMC results, we used deposition parameters close to the values typically used in experiments: 0.08 ML of atoms were deposited with rate 0.002 ML s^{-1}. Temperature was set to 300 K. A frequency prefactor value of 10^{13} s^{-1} was used. Array of 512×512 positions with periodic boundary conditions was used for calculation. If necessary (small volume of statistical data in case of large island growth), averaging over several runs was performed.

III. RESULTS AND DISCUSSION

A. Irreversible growth with anisotropic diffusion

1. Model without prohibited zones

Figure 2(a) (squares) shows the island size distribution simulated by the kMC model with highly anisotropic diffusion parameters ($E_{\parallel}=0.4$ eV and $E_{\perp}=0.81$ eV for comparison to Ref. [3]) and without reactive defects. Irreversibility is assured by setting E_{attr} to a high value, so that no decay of islands takes place during simulation. Repulsion energy was set $E_{rep}=0.8$ eV. The distribution is monomodal as usual in a standard irreversible growth by aggregation of diffusing adatoms [16,17]. The corresponding concentration of islands is $N=\Sigma N(s)=0.0024$ ML where $N(s)$ is concentration of islands with a size of s. A change in the distribution when reactive defects are placed on the surface prior to deposition of adatoms is shown in Fig. 2(b) and 2(c). In Fig. 2(b), defect concentration (defined as ratio of number of defects and number of available sites) is 0.0025 ML, which is comparable to the island concentration N after deposition of the same coverage on the surface without defects; in Fig. 2(c) the defect concentration is doubled, 0.005 ML. The defect concentration of 0.0025 ML [Fig. 2(b)] results in a significant change in the island size distribution—number of small islands increases and the distribution is monotonically decreasing. With increasing concentration of defects the distribution decreases more steeply with s and at a value of 0.005 ML becomes exponential [dashed line in Fig. 2(c)]. The Fig. 2 shows that monotonicity of the size distribution can be reached as result of presence of reactive defects without introducing prohibited zones to the model.

This finding is opposite to the result of Ref. [13], in which it is argued that defects could not be responsible for monotonicity of size distribution. The main reasons mentioned in

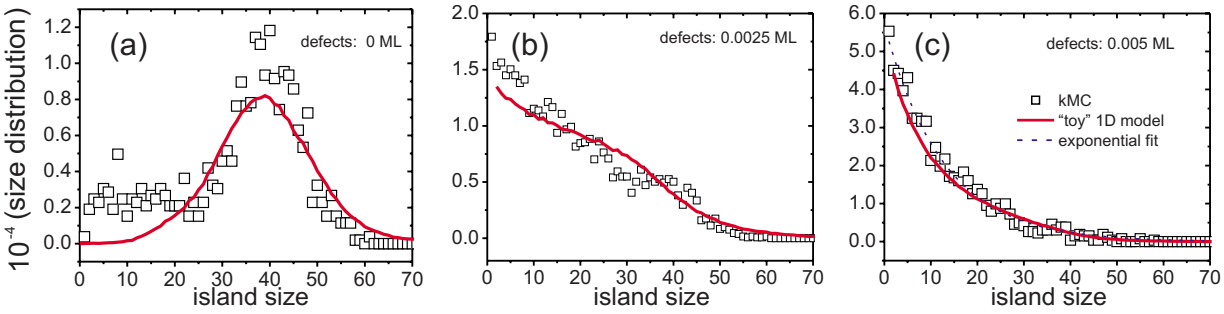

FIG. 2. (Color online) Island size distributions obtained by kMC simulation using the anisotropic irreversible model without prohibited zones (squares) and by a simple 1D "toy" model (solid lines). Concentration of reactive defects on the surface is 0 (a), 0.0025 (b), and 0.005 ML (c). With increasing defect concentration, the distribution changes from monomodal to exponentially decreasing. The exponential fit is shown in (c) by dashed line.

[13] are: (i) at observed concentration of the defects (0.003 ML) just about half of islands nucleated on the defects, which makes the effect significant but not dominant; (ii) a strong influence of defects is limited to islands with weak bonding between adatoms; (iii) if the defects represent nucleation sites, island size distribution would reflect the size distribution of corresponding capture zones, which is monomodal. Next we discuss all points listed above in the view of our results. (i) At defect coverage of 0.0025 ML (see Fig. 3), island density is 0.0044 ML, of which 0.0024 ML (0.0020 ML) are terminated (not terminated) by defects. It means that ~55% of islands are nucleated on defects, the rest is "self-nucleation," which is comparable to [13]. Yet, the distribution is monotonically decreasing, as shown in Fig. 2(b). A model explaining the calculated distribution is discussed below. (ii) Even in the case of irreversible growth (Fig. 2) the distribution becomes monotonically decreasing upon introducing defects. Fast diffusion (in one direction) compared to deposition rate allows adatoms to find reactive defects in amount sufficient for qualitative change in the distribution function. (iii) The size (area) distribution of capture zones of randomly deposited defects on the surface is monomodal in the two-dimensional case. However, in a strongly anisotropical system (as the studied one) the capture zones are rather one-dimensional. Then, the size (length) distribution of the capture zones is exponentially decreasing, as we further discuss in this section.

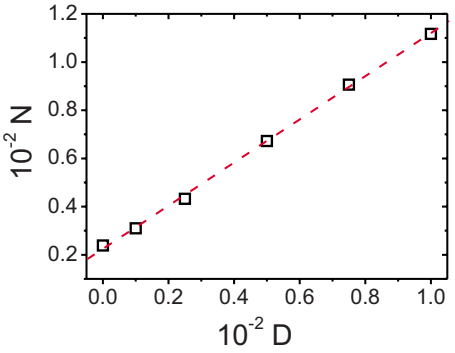

FIG. 3. (Color online) Dependence of concentration of islands on concentration of reactive defects (squares). Dashed line is a linear fit. Data obtained from kMC simulations using an anisotropic irreversible model without prohibited zones.

Growth with nucleation on defects is in a way analogical to growth with nuclei created by irreversible reaction with atoms of the substrate [24]. In that case, defect concentration (probability of finding a defect) is replaced by probability of the reaction with a substrate atom. The important difference is that number of defects available is decreasing during the growth, while number of sites available to the reaction with substrate atoms [24] is almost constant in the low coverage regime. In both cases, the size distribution is monotonically decreasing.

The concentration of islands N depends linearly on concentration of defects D, as shown in Fig. 3 (squares). A slope of the linear fit (dashed line) is 0.9 and in the studied regime about 90% of defects are occupied by islands independently on defect concentration.

Furthermore, we discuss in detail a reason of a change in the island size distribution in case of surface with defects [Figs. 2(a)–2(c)]. The activation energies used in the above simulation correspond to strongly anisotropic diffusion. A degree of the anisotropy can be defined as a ratio of the relative jump rates in parallel and perpendicular directions, respectively, $R_{\parallel}/R_{\perp}=\exp[(E_{\perp}-E_{\parallel})/\mathrm{kT}]\approx 8\times 10^{6}$ at room temperature. Considering a free isolated adatom, the corresponding average diffusion distance (parallel with islands) between two consecutive jumps in the perpendicular direction would be $\sqrt{R_{\parallel}/R_{\perp}}\approx 3000$ positions, which is comparable to a common width of a terrace on real surfaces experimentally observed. We assume that due to the high anisotropy, the two-dimensional surface can be reduced to a one-dimensional representation: 1D array of sites which can be empty or occupied either by an adatom or by a defect. To mimic the C-type defects on Si(100) surface, one side of each defect is randomly selected as reactive and the opposite one as inert [23]. Random deposition of the defects divides the 1D array into "boxes" separated by the defects. From the basic probability theory, distribution of the box length b is $\lambda \exp(-\lambda b)$, where λ is the number of boxes per unit length. Adatoms impinging to such a box cannot escape. Assume that all atoms deposited to a particular box aggregate and form an island (we call such case the limit of fast diffusion). Then, a size of the island formed in the box is proportional to the length of the box, because on average $F\times b$ atoms impinge into the box of length b, where F is the deposition flux. Finally, the island size distribution is proportional to the ini-

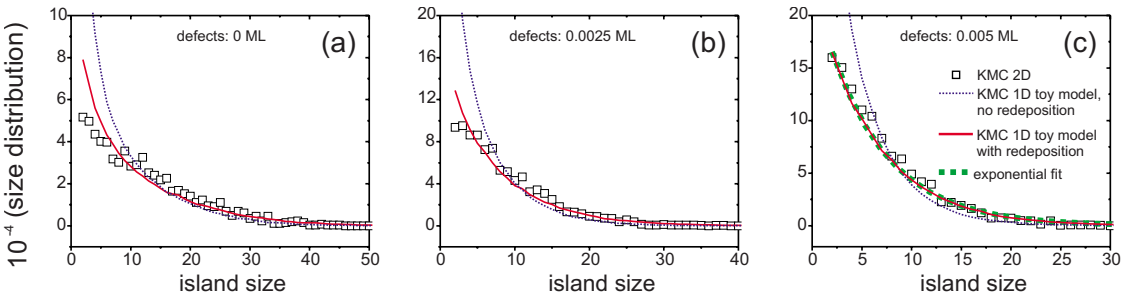

FIG. 4. (Color online) Island size distributions obtained by kMC simulation using anisotropic irreversible model with prohibited zones (squares), compared to results of 1D "toy model" (dotted lines) and to 1D "toy" model using redeposition of adatoms (solid lines). Concentration of reactive defects on the surface is 0 (a), 0.0025 (b), and 0.005 ML (c). Slope of the distribution increases with concentration of the defects. Exponential fit is shown in (c) by dashed line.

tial distribution of box length, i.e., exponentially decaying.

In order to test a validity of the used simplification—restriction to 1D model and the limit of fast diffusion—we used a simple "toy" Monte Carlo model. Initially, the surface is represented by a 1D array of sites onto which defects are randomly distributed. During growth, the only parameter representing diffusion is a length of 1D capture zone l_C—all atoms deposited into the zone (within the distance l_C from a reactive defect or island) are trapped by this reactive site. In more detail, the following steps are repeated: (i) an adatom is randomly deposited, (ii) if there is a reactive defect or island in a distance $l<l_C$ from the deposited adatom, the adatom attaches to the nearest of such positions, otherwise, a new island of size 1 is established. The simulation terminates when desired coverage θ is reached. The results of the "toy" simulations (obtained with fitted value of $l_C=460$) are compared to kMC "exact" simulations in Figs. 2(a)–2(c) (solid lines). A very good agreement demonstrates that the simplifications used in the "toy" model are justified for the studied case. Figure 2(b) represents a critical situation when l_C is comparable to average spacing between neighboring defects D^{-1}, where D is the concentration of defects. If $l_C \gg D^{-1}$ [Fig. 2(c)], all adatoms deposited into a box surrounded by two defects belong to the same capture zone and create a single island. Thus, the limit of infinite diffusion is reached by the defect concentration even if ratio of hopping rate and deposition flux is finite.

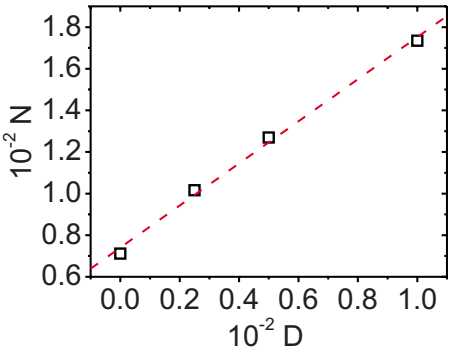

FIG. 5. (Color online) Dependence of concentration of island on concentration of reactive defects (squares). Dashed line is a linear fit. Results of kMC simulation using anisotropic irreversible model with prohibited zones.

2. Model with prohibited zones

The monotonically decreasing size distribution of Ga islands was previously obtained as a result of a model with strongly anisotropic diffusion in combination with prohibited zones [3]. Albao *et al.* obtained a good agreement with their experimental data for diffusion barriers $E_{\parallel}=0.4$ eV and $E_{\perp}=0.81$ eV (for parallel and perpendicular diffusion, respectively). Concentration of diffusing (free) atoms in such a case is high and nucleation of new islands is enhanced.

Figure 4 (squares) shows the influence of increasing defect concentration, as calculated by the kMC model, after introducing prohibited zones [3]. All parameters are set the same as used to calculate data shown in Fig. 2. Compared to the model without prohibited zones (Fig. 2), a higher amount of smaller islands is formed. Due to the adatom repulsion from the prohibited zones (marked by arrows in Fig. 1) attachment of adatoms is limited. Considering the anisotropic diffusion, deposited adatoms can be trapped in a gap between two prohibited zones (marked by asterisk in Fig. 1). The trapped atom cannot attach to any of the existing islands until it jumps in perpendicular direction (which is a rare event due to the large diffusion barrier in this direction) or another atom is randomly deposited to the gap. The resultant island concentration N is shown in Fig. 5 (squares) as a function of defect concentration. The dependence is linear (dashed line) with slope close to 1.0.

In the kMC model described above, there are two zones prohibited for diffusing atoms along each 1D island (the prohibited zones are marked by the crosses in Fig. 1). The zones can be effectively introduced to the "toy" 1D model by generating two zones per a new nucleated island at random positions within the 1D array (see the process marked "A" in Fig. 6 for illustration). Results of such simulations are shown

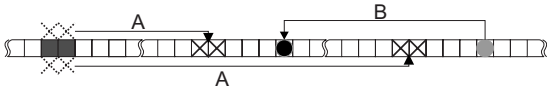

FIG. 6. Schematic illustration of processes used in the "toy" 1D model. Arrow marked "A"—formation of prohibited zones (crosses) at random positions when new island nucleates. Dotted crosses show positions where the prohibited zones would appear in a 2D model. Arrow marked "B"—random redeposition of adatom (ball) simulating jumps between adjacent rows.

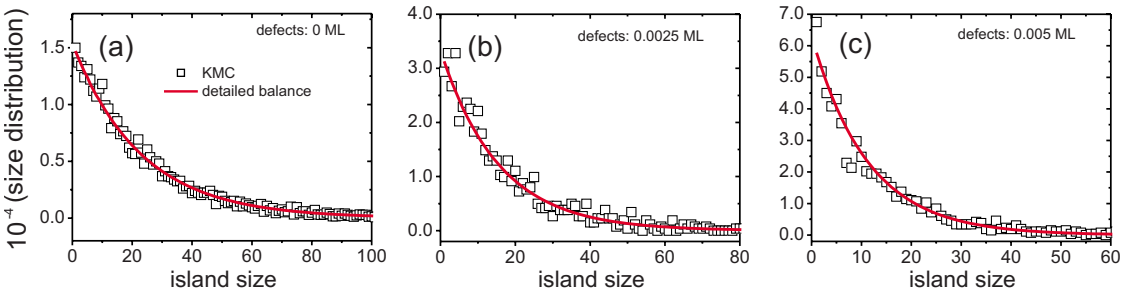

FIG. 7. (Color online) Island size distributions obtained by kMC simulation using the close-to-equilibrium model (squares), compared to analytical solution (solid lines). Concentration of reactive defects on the surface is 0 (a), 0.0025 (b), and 0.005 ML (c).

in Fig. 4 (dotted line), the agreement is not very good. An explanation is that the 1D simplification fails when prohibited zones are introduced—jumps of adatoms trapped between two prohibited zones take place even if time constant of such a process is high (≈ 4 s when $E_{\perp}=0.81$ eV). Such escape jumps can be effectively modeled by random redeposition (removing and depositing again) of an adatom, as schematically illustrated in Fig. 6 by the arrow "B." Indeed, after introducing the random escape with a time constant of 4 s to the "toy" model, a better agreement with kMC is obtained (Fig. 4, solid lines). The agreement confirms that low rate processes can be introduced to the toy model without need of "exact" hopping event-based kMC simulation, which usually requires significant computational time, especially in the case of highly diffusive atoms.

B. Close-to-equilibrium model

In this section, we consider systems with decaying islands growing on the substrate by means of reversible processes. If allowed to relax sufficiently long time, a morphology does not depend on preparation condition (deposition rate). For atoms of group III elements deposited on Si(100) decay of islands at room temperature was reported in the case of In [4,23] and Tl [1,2]. On a perfect substrate, monotonically decreasing size distribution was reported as a result of thermal equilibrium reached by reversible processes [8,10]. In case of the equilibrium, all competing processes are in balance and the island size distribution can be derived analytically with a good approximation for low coverages (≤ 0.1 ML). A detailed balance condition gives

$$N(s+1)\nu_{DET} = N(1)N(s)\nu_{ATT}, \tag{3}$$

where $N(s)$ is the number of islands of size s, ν_{DET} is the detachment rate and ν_{ATT} is the attachment rate, i.e., the rate of jumps to a position where atom is bonded to an island. The left side of Eq. (3) represents decay rate of islands of size $s+1$ and the right side represents growth rate of islands of size $s+1$ by means of attachment of diffusing adatom to islands of size s. The condition of detailed balance results in expression for the distribution $N(s)$

$$N(s) = N(1)\left[N(1)\frac{\nu_{ATT}}{\nu_{DET}}\right]^{(s-1)} = \frac{\nu_{DET}}{\nu_{ATT}}\exp\left[s \times \ln\left(N(1)\frac{\nu_{ATT}}{\nu_{DET}}\right)\right]. \tag{4}$$

From a normalization condition $\Sigma sN(s)=\theta$, where θ is the coverage, $N(1)$ can be calculated,

$$N(1) = [\alpha + 1 - \sqrt{2\alpha+1}]/(\alpha\nu_{ATT}/\nu_{DET}), \tag{5}$$

where $\alpha = 2\theta\nu_{ATT}/\nu_{DET}$. Evidently, the distribution $N(s)$ is always monotonically decreasing in the case of thermal equilibrium.

It should be noted that the distribution $N(s)$ depends for given θ only on the ratio ν_{ATT}/ν_{DET}. The rates ν_{ATT} and ν_{DET} can be calculated using Eq. (1) with activation energies for diffusion (E_{dif}) and atom detachment ($E_{det}=E_{dif}+E_{attr}$), respectively. For the identical frequency prefactors of both thermally activated processes, we obtain $\nu_{ATT}/\nu_{DET} = \exp[(E_{det}-E_{dif})/kT] = \exp[E_{attr}/kT]$. In the other words, the distribution $N(s)$ depends only on bonding energy between the nearest neighbors in the 1D island. Thus, diffusion parameters of free adatoms (hopping rates) do not influence the distribution of island size, once equilibrium is reached (but the time of establishing the equilibrium depends of course on the diffusion parameters). This is in agreement with results derived from thermodynamical consideration of the relaxing system previously [10].

In Fig. 7(a), kMC results are compared to an analytical solution of Eq. (4). In the kMC simulation, the activation energies were calculated using Eq. (2). Energy of NN atom interaction within an island was set to $E_{attr}=E_{det}-E_{dif} = 0.22$ eV in both cases, the same as the value used in Refs. [8,10]. Values of diffusion parameters $E_{\parallel}=0.64$ eV and $E_{\perp} = 0.62$ eV were taken from Ref. [8] and deposited islands were allowed to relax 3 h after deposition at room temperature. A good agreement of kMC and analytical distributions confirms that the simulated morphologies are close to the thermal equilibrium.

Next, we focus on influence of reactive defects on the distribution in the thermal equilibrium. Figures 7(b) and 7(c) show kMC results for different concentrations of defects, 0.0025 (b) and 0.005 ML (c). The monotonically decreasing character is preserved, slope of the distribution is steeper in the case of higher defect concentration. Resulting dependence of island density N on defect concentration is linear with slope 0.65, as shown in Fig. 8.

The balance condition [Eq. (3)] can be modified for a system with the defects. The distribution is divided into two parts corresponding to a population of islands pinned by defects, $N_d(s)$, and nonpinned islands, $N_n(s)$, respectively. The detailed balance condition is expressed by equations

$$N_n(s+1)\nu_{DET} = N_n(1)N_n(s)\nu_{ATT}, \tag{6}$$

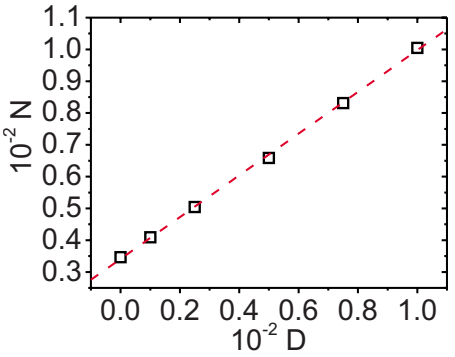

FIG. 8. (Color online) Island concentration as function of concentration of reactive defects simulated by kMC simulation using the close-to-equilibrium model (squares). Dashed line is a linear fit.

$$N_d(1)\nu_{2DET} = N_n(1)N_{\text{free}D}\nu_{ATT}, \tag{7}$$

$$N_d(s+1)\nu_{DET} = N_n(1)N_d(s)\nu_{ATT}, \tag{8}$$

where ν_{2DET} is the detachment rate of an adatom from a defect, and N_{freeD} is the concentration of defects not occupied by islands. Normalization conditions are $\Sigma sN_n(s) + \Sigma sN_d(s) = \theta$, and $D = \Sigma N_d(s) + N_{freeD}$, where D is the defect concentration. Resulting distributions for both N_n and N_d are again exponentially decaying for $N_d \geq 2$. The distributions $N_n(s) + N_d(s)$ calculated for different defect concentrations are compared to kMC simulations in Figs. 7(b) and 7(c).

In our kMC simulations, we use a high value of interaction energy between a defect and an island, in agreement with experiment and ab-initio calculation [23]. In such case, $\nu_{2DET} \rightarrow 0$ and all defects become occupied by islands in equilibrium, $N_{freeD} = 0$. We note that for higher defect concentrations ($\sim$0.01 ML), some of the defects ($\sim$10%) randomly placed on 2D lattice are so close to each other that some of pinned islands would grow in unfavored proximity with spacing of a in the $\perp$ direction. Therefore, number of "active" defects is then lower than D.

It is interesting to mention that distributions obtained for surface with $\geq$0.005 ML of reactive defects are in fact the same in the case of irreversible anisotropic aggregation [Fig. 2(c)] and in the case of the equilibrium system [Fig. 7(c)]. The presence of the reactive defects may suppress differences between results of the different models. It demonstrates a need of a careful interpretation of experimental data obtained for growth at presence of surface defects. For the correct interpretation, experimental data additional to island size distribution are required, e.g., size fluctuation of selected islands.

IV. CONCLUSION

Two different models of 1D island growth were used to study an influence of reactive defects on size distribution of islands—the irreversible model with anisotropic diffusion and the equilibrium model with balance between attachment and detachment of atoms. In the case of the irreversible model, a nontrivial single-parameter simplification to 1D model with capture zones was applied, sufficiently reproducing "exact" results of kMC simulation. If average defect spacing is smaller than size of the capture zone ($\sim 5 \times 10^2$ in the studied case), the growth becomes controlled by the defect concentration only. The distribution of island size changed from monomodal to monotonically decreasing at concentration of defects comparable to density of islands on the surface without defects (0.0025 ML of defects for deposited amount 0.08 ML). In the case of the equilibrium model, we derived an analytical solution of island size distribution taking into account preferred nucleation on defects. Independently on defect concentration, the distribution is exponential. At a defect concentration of 0.005 ML, irreversible and equilibrium models give a similar island size distributions, depending only on amount of atoms and defects deposited on the surface.

ACKNOWLEDGMENTS

This work is a part of the research plan Grant No. MSM 0021620834 that is financed by the Ministry of Education of the Czech Republic and was partly supported by Project No. 100907 of GAUK.

[1] M. Kishida, A. Saranin, A. Zotov, V. Kotlyar, A. Nishida, Y. Murata, H. Okado, M. Katayama, and K. Oura, Appl. Surf. Sci. **237**, 110 (2004).
[2] A. A. Saranin *et al.*, Phys. Rev. B **71**, 035312 (2005).
[3] M. A. Albao, M. M. R. Evans, J. Nogami, D. Zorn, M. S. Gordon, and J. W. Evans, Phys. Rev. B **72**, 035426 (2005).
[4] P. Kocán, P. Sobotík, I. Ošt'ádal, J. Javorský, and M. Setvín, Surf. Sci. **601**, 4506 (2007).
[5] P. Gambardella, M. Blanc, H. Brune, K. Kuhnke, and K. Kern, Phys. Rev. B **61**, 2254 (2000).
[6] P. Gambardella, M. Blanc, L. Bürgi, K. Kuhnke, and K. Kern, Surf. Sci. **449**, 93 (2000).
[7] P. Gambardella, H. Brune, K. Kern, and V. I. Marchenko, Phys. Rev. B **73**, 245425 (2006).
[8] J. Javorský, M. Setvín, I. Ošt'ádal, P. Sobotík, and M. Kotrla, Phys. Rev. B **79**, 165424 (2009).
[9] V. I. Tokar and H. Dreyssé, Phys. Rev. E **68**, 011601 (2003).
[10] V. I. Tokar and H. Dreyssé, Phys. Rev. B **74**, 115414 (2006).
[11] R. B. Stinchcombe and F. D. A. Aarão Reis, Phys. Rev. B **77**, 035406 (2008).
[12] S. Jun, H. Zhang, and J. Bechhoefer, Phys. Rev. E **71**, 011908 (2005).
[13] M. A. Albao, M. M. R. Evans, J. Nogami, D. Zorn, M. S. Gordon, and J. W. Evans, Phys. Rev. B **74**, 037402 (2006).
[14] G. Brocks, P. J. Kelly, and R. Car, Phys. Rev. Lett. **70**, 2786 (1993).
[15] I. Ošt'ádal, J. Javorský, P. Kocán, P. Sobotík, and M. Setvín, J. Phys.: Conf. Ser. **100**, 072006 (2008).

[16] M. C. Bartelt and J. W. Evans, Phys. Rev. B **46**, 12675 (1992).
[17] C. Ratsch and J. A. Venables, J. Vac. Sci. Technol. A **21**, S96 (2003).
[18] F. Slanina and M. Kotrla, Physica A **256**, 1 (1998).
[19] M. Z. Hossain, Y. Yamashita, K. Mukai, and J. Yoshinobu, Phys. Rev. B **67**, 153307 (2003).
[20] S. Okano and A. Oshiyama, Surf. Sci. **554**, 272 (2004).
[21] S.-Y. Yu, H. Kim, and J.-Y. Koo, Phys. Rev. Lett. **100**, 036107 (2008).
[22] P. Kocán, P. Sobotík, and I. Ošt'ádal, Phys. Rev. B **74**, 037401 (2006).
[23] P. Kocán, L. Jurczyszyn, P. Sobotík, and I. Ošt'ádal, Phys. Rev. B **77**, 113301 (2008).
[24] D. D. Chambliss and K. E. Johnson, Phys. Rev. B **50**, 5012 (1994).